Journal of Sound and Vibration (2001) **247**(5), 835–856
doi:10.1006/jsvi.2001.3753, available online at http://www.idealibrary.com on IDEAL®

ON COUPLED LONGITUDINAL AND LATERAL VIBRATIONS OF ELASTIC RODS

O. M. O'Reilly

Department of Mechanical Engineering, University of California, Berkeley, CA 94720-1740, *U.S.A.*

(*Received* 6 *November* 2000, *and in final form* 17 *April* 2001)

In this paper, the coupled longitudinal and lateral vibrations of a rectangular parallelepiped composed of a uniform, isotropic, elastic body are examined. The one-dimensional model for the body was developed by Green, Naghdi and several of their co-workers. It is based on a Cosserat or directed rod theory. The frequency spectrum is found to divide naturally into three regions which are separated by degenerate cases. When the cross-section of the body is square, a natural splitting of the modes occurs. One-half of this split involves motions coupling the axial extension and symmetric lateral deformation of the body. The other half involves asymmetric lateral deformations. The cases of a free–free rod and a cantilevered rod are discussed and the results compared to existing works in the literature which use the three-dimensional theory of elasticity to model the vibrations.

1. INTRODUCTION

The vibrations of three-dimensional rod-like bodies has attracted a significant number of works which can be classified into two categories. The first category uses the three-dimensional theory of linear elasticity to determine these vibrations, while the second employs one-dimensional theories of rods. Arguably, the most famous contributions in this area are the works of Pochhammer and Chree in the 19th century. They investigated travelling waves in infinitely long cylindrical bodies (see references [1, 2], and references therein), and their solutions have become benchmarks for all other works on this topic. However, if the rod-like body is finite or does not have a cylindrical cross-section, then exact solutions from the three-dimensional theory appear to be impossible to obtain in all but a handful of cases. These difficulties have inspired a vast amount of work both in the development of approximate solutions to the three-dimensional theory and in the development of one-dimensional models based on rod theories. The latter models have certain tractible features which render them suitable for design studies.

Despite the considerable amount of research on wave propagation and vibration of rods, there is surprisingly little research on coupled longitudinal and lateral vibrations of rod-like bodies with rectangular cross-sections. Specifically, Chree [3] in 1889 discussed an approximate dispersion relation for long wavelength modes in an infinitely long body with an arbitrary cross-section. Later, Morse [4, 5] and Kynch and Green [6] examined this problem for rectangular cross-sections. Most of their results pertain to large wavelength vibrations. For parallelepipeds of finite length, and using the three-dimensional theory of linear elasticity, exact solutions were obtained for certain cases by Lamé [7] and Mindlin [8, 9] and approximate solutions have been obtained by Ekstein and Schiffman [10], Hutchinson and Zillmer [11], Leissa *et al.* [12, 13], and Lim [14]. Recently, Rubin [15] employed his theory of a Cosserat point to examine this problem.

0022-460X/01/450835 + 22 $35.00/0

In the context of rod theories, the most commonly used model is the (one-dimensional) wave equation:

$$c_0^2 \frac{\partial^2 u_3}{\partial x_3^2} = \frac{\partial^2 u_3}{\partial t^2}, \tag{1}$$

where u_3 is the longitudinal displacement and c_0 is the bar wave speed. This model, however, does not incorporate lateral displacements. To this end, Love developed a model which incorporates the inertia of these displacements (cf. section 278 of reference [1]):

$$c_0^2 \left(\frac{\partial^2 u_3}{\partial x_3^2} + \nu^2 k^2 \frac{\partial^4 u_3}{\partial t^2 \partial x_3^2} \right) = \frac{\partial^2 u_3}{\partial t^2}, \tag{2}$$

where ν is the Poisson ratio and k is the polar radius of gyration of the cross-section. A more accurate model was developed by Green and Nagdhi and several of their co-workers as a particular case of their rod theory [16–21]. This rod theory was the basis for a study of these motions in rods with rectangular cross-sections by Turcotte [22] and Krishnaswamy and Batra's work in references [23–25] for rods with circular cross-sections.† In the present paper, Green and Naghdi's rod theory is also used to study the vibrations, and Turcotte's results are significantly extended. One of the motivations for examining the coupled longitudinal and lateral vibrations lies in extending several recent studies of the steady motions of rods (cf. references [27, 28]). As a precursor to examining the linear stability of these motions, it is necessary to examine the vibrational response of the rest state. The developments of the present paper address this matter.

Since the model used here is not very well known, section 2 of this paper is partially devoted to supplying the relevant background. There, it is necessary to alter some of the constitutive prescriptions commonly used in order to match certain dynamic solutions of this theory with those from three-dimensional considerations. Next, in section 3, the free-vibrations problem for the model is discussed and various intermediate results are established. These results show that the frequency spectrum is split into three by the presence of two degenerate cases. These cases are similar to the thickness-shear mode observed in Timoshenko's beam theory (see references [29, 30], and references therein). Section 4 is devoted to the special case of a square cross-section. For this case, the governing equations split into two sets. One of these sets is similar to the equations considered by Mindlin and Herrmann [26] and Krishnaswamy and Batra [23], while the other set governs asymmetric vibrations of the cross-sections. Prescriptions for three constants appearing in the model are presented in section 5. These prescriptions are based on the works of Rubin [15, 31] and Mindlin and Deresiewicz [32]. To illustrate the predictions of the model, the case of a free–free rod with a rectangular cross-section is discussed in section 6, while a rod with a square cross-section is discussed in section 7. In section 8, the case of a fixed–free (or cantilevered) rod is considered. The closing section of the paper discusses actuation of the vibrations.

2. APPLICATION OF A DIRECTED ROD THEORY

Dating to a seminal paper by Green and Laws [16], Green, Naghdi and several of their co-workers developed a theory for deformable rod-like bodies. In this theory, the rod is

†Krishnaswamy and Batra's model for these vibrations is similar to one proposed by Mindlin and Herrmann [26].

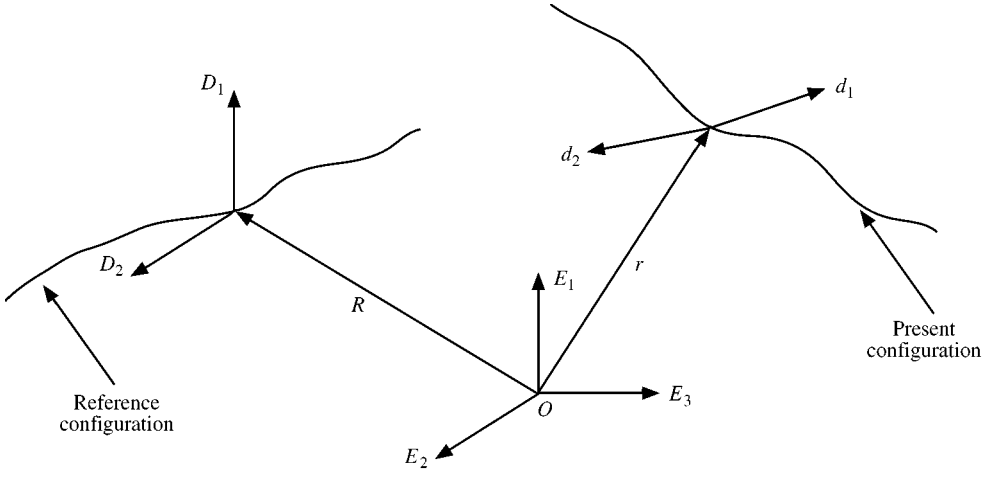

Figure 1. The reference and present configurations of a directed curve. The present configuration is defined by the functions $\mathbf{r}(\xi, t)$, $\mathbf{d}_1(\xi, t)$, and $\mathbf{d}_2(\xi, t)$, while the reference configuration is defined by the functions $\mathbf{R}(\xi)$, $\mathbf{D}_1(\xi)$, and $\mathbf{D}_2(\xi)$. In this figure, the values of these functions for a particular material point of the directed curve are shown.

modelled using a directed curve. This is a material curve to which, at each material point, a set of deformable vector fields (known as directors) are associated. As discussed in references [20, 21], the theory extended the earlier work of the Cosserat brothers by allowing an arbitrary number of deformable directors. A unique feature of this theory is the ability to model lateral expansion and contraction of the rod-like body.‡

For the purpose of the present paper, interest is restricted to a rod theory where two director fields, $\mathbf{d}_1$ and $\mathbf{d}_2$, are present. Referring to Figure 1, the reference configuration of the body is modelled using a directed curve. The material points of this curve are uniquely identified by the co-ordinate ξ, and their position vectors are defined by the function $\mathbf{R} = \mathbf{R}(\xi)$. The directors associated with a material point in this configuration are defined by the functions $\mathbf{D}_1 = \mathbf{D}_1(\xi)$ and $\mathbf{D}_2 = \mathbf{D}_2(\xi)$. In the present configuration, the position vector of the material points are defined by $\mathbf{r} = \mathbf{r}(\xi, t)$, while the directors are defined by $\mathbf{d}_1 = \mathbf{d}_1(\xi, t)$ and $\mathbf{d}_2 = \mathbf{d}_2(\xi, t)$.

It is also useful to recall the correspondences between the position vectors of material points of the rod-like body in its reference and present configurations to related quantites for the directed curve. To this end, let $(\xi, \theta^1, \theta^2)$ be a co-ordinate system for the fixed region of space occupied by the body in its reference configuration. Then, the fixed directors can be chosen such that, in the reference configuration,

$$\mathbf{R}^* = \mathbf{R}^*(\xi, \theta^1, \theta^2) = \mathbf{R} + \theta^1 \mathbf{D}_1 + \theta^2 \mathbf{D}_2. \tag{3}$$

In the present configuration of the rod-like body, the following approximation is assumed to hold:

$$\mathbf{r}^* = \mathbf{r}^*(\xi, \theta^1, \theta^2, t) = \mathbf{r} + \theta^1 \mathbf{d}_1 + \theta^2 \mathbf{d}_2. \tag{4}$$

Consequently, the directors can be considered to account for the deformation of material fibers in the cross-sections of the body.

‡This feature is also important in modeling problems involving contact (see references [33, 28]).

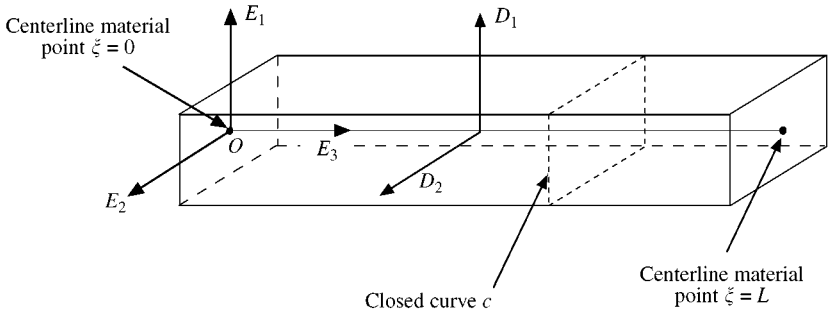

Figure 2. A fixed reference configuration of a rod-like body. The region of space occupied by the body has a length L, width w, and height h. The reference configuration of the material curve associated with the directed curve is also shown in this figure. This curve is chosen to be the (length-wise) centerline of the body. The curve c shown in the figure will be used later in prescribing applied forces.

To determine the fields $\mathbf{r}(\xi, t)$, $\mathbf{d}_1(\xi, t)$, and $\mathbf{d}_2(\xi, t)$, balance laws and constitutive relations are postulated. After some reductions, a set of partial differential equations for these fields are obtained. These laws are not presented in all their generality here, instead they are specialized to the rod-like body of interest. Specifically, of interest in this paper is a body whose reference configuration is of the form of a parallelepiped of length L which has a cross-section of height h and width w. This body is assumed to be composed of a homogeneous, isotropic, linearly elastic material.

One denotes by x_i and $\mathbf{E}_i$ a Cartesian co-ordinate system and its associated right-handed orthonormal basis vectors for $\mathscr{E}^3$. As shown in Figure 2, the ξ co-ordinate coincides with the x_3 co-ordinate, while $\theta^1 = x_1$ and $\theta^2 = x_2$. In addition, the directors are chosen such that $\mathbf{D}_1 = \mathbf{E}_1$ and $\mathbf{D}_2 = \mathbf{E}_2$. The motion of the directed curve is assumed to be such that

$$\mathbf{r} - \mathbf{R} = u_3 \mathbf{E}_3, \quad \mathbf{d}_1 - \mathbf{D}_1 = \delta_{11} \mathbf{E}_1, \quad \mathbf{d}_2 - \mathbf{D}_2 = \delta_{22} \mathbf{E}_2, \tag{5}$$

where the longitudinal displacement, u_3, and lateral displacements, δ_{11} and δ_{22}, are functions of t and ξ. In the infinitesimal (or linear) theory of interest here, the spatial and time derivatives of the displacements are assumed to be small.

In the presence of body forces and tractions on the lateral surface of the rod-like body, Green and Naghdi [19] have shown that the longitudinal and lateral displacements of the rod are governed by the following balance laws:

$$\frac{\partial n_3}{\partial \xi} + \lambda f_3 = \lambda \frac{\partial^2 u_3}{\partial t^2}, \quad \frac{\partial m_{11}}{\partial \xi} - k_{11} + \lambda l_{11} = \lambda y^{11} \frac{\partial^2 \delta_{11}}{\partial t^2}, \quad \frac{\partial m_{22}}{\partial \xi} - k_{22} + \lambda l_{22} = \lambda y^{22} \frac{\partial^2 \delta_{22}}{\partial t^2}. \tag{6}$$

In these equations, $\xi = x_3$ is the arc-length parameter of the rod in a fixed reference configuration, λ is the mass per unit length of ξ, and y^{11} and y^{22} are inertial coefficients. For the rod theory of interest, one also has the contact force, $\mathbf{n}$, intrinsic contact forces, $\mathbf{k}^1$ and $\mathbf{k}^2$, and contact director forces, $\mathbf{m}^1$ and $\mathbf{m}^2$. Constitutive relations are required for these forces. The applied force $\lambda \mathbf{f}$ and applied director forces, $\lambda \mathbf{l}^1$ and $\lambda \mathbf{l}^2$, represent the combined contributions of body forces and tractions on the lateral surface of the rod-like body. In the balance laws discussed above, certain components of the various forces are present: $n_3 = \mathbf{n} \cdot \mathbf{E}_3$, $f_3 = \mathbf{f} \cdot \mathbf{E}_3$, $m_{11} = \mathbf{m}^1 \cdot \mathbf{E}_1$, $m_{22} = \mathbf{m}^2 \cdot \mathbf{E}_2$, $k_{11} = \mathbf{k}^1 \cdot \mathbf{E}_1$, $k_{22} = \mathbf{k}^2 \cdot \mathbf{E}_2$, $l_{11} = \mathbf{l}^1 \cdot \mathbf{E}_1$, and $l_{22} = \mathbf{l}^2 \cdot \mathbf{E}_2$.

The solution of equations (6) depends on the initial conditions $u_3(\xi, t_0)$, $\delta_{11}(\xi, t_0)$, and $\delta_{22}(\xi, t_0)$. In addition, six boundary conditions need to be prescribed. For example, for a rod which is clamped at the end $\xi = 0$ and traction-free at the end $\xi = L$, the boundary conditions at the fixed end are

$$u_3(\xi = 0, t) = 0, \qquad \delta_{11}(\xi = 0, t) = 0, \qquad \delta_{22}(\xi = 0, t) = 0, \tag{7}$$

while, at the other end of the rod,

$$n_3(\xi = L, t) = 0, \qquad m_{11}(\xi = L, t) = 0, \qquad m_{22}(\xi = L, t) = 0. \tag{8}$$

It should be noted that these and other boundary conditions can be inferred using known correspondences between the rod theory of interest here and three-dimensional continuum mechanics (see, for example, references [19] or [34]).

Assuming a linear isotropic elastic rod-like body with rectangular cross-sections, the constitutive equations for the force components n_3, m_{11}, m_{22}, k_{11}, and k_{22} are

$$m_{11} = \alpha_{10}\frac{\partial \delta_{11}}{\partial \xi} + \alpha_{17}\frac{\partial \delta_{22}}{\partial \xi}, \qquad m_{22} = \alpha_{17}\frac{\partial \delta_{11}}{\partial \xi} + \alpha_{11}\frac{\partial \delta_{22}}{\partial \xi},$$

$$k_{11} = \alpha_1\delta_{11} + \alpha_7\delta_{22} + \alpha_8\frac{\partial u_3}{\partial \xi}, \qquad k_{22} = \alpha_7\delta_{11} + \alpha_2\delta_{22} + \alpha_9\frac{\partial u_3}{\partial \xi},$$

$$n_3 = \alpha_8\delta_{11} + \alpha_9\delta_{22} + \alpha_3\frac{\partial u_3}{\partial \xi}. \tag{9}$$

For a rectangular rod of mass density ρ_0, height h, width w, Young's modulus E, and the Poisson ratio v, it is recalled, from reference [19], that

$$\alpha_1 = \alpha_2 = \alpha_3 = \frac{EA(1-v)}{(1+v)(1-2v)}, \qquad \alpha_7 = \alpha_8 = \alpha_9 = \frac{EAv}{(1+v)(1-2v)},$$

$$\alpha_{10} = \frac{EI_2}{2(1+v)}, \qquad \alpha_{11} = \frac{EI_1}{2(1+v)}, \qquad \alpha_{17} = 0, \tag{10}$$

where $A = hw$, $I_1 = w^3h/12$, and $I_2 = h^3w/12$. Prescriptions (10) are motivated by comparing static solutions of the balance laws with corresponding solutions from the three-dimensional theory of elasticity.

In the works of Green and Naghdi, it is standard to specify

$$\lambda = \rho_0 A, \qquad \lambda y^{11} = \rho_0 I_2, \qquad \lambda y^{22} = \rho_0 I_1. \tag{11}$$

However, these prescriptions will not yield good agreement between the vibrational response of the rod and three-dimensional results. In this paper, an idea of Rubin [15, 31] is used and these coefficients are chosen to match corresponding results from the three-dimensional theory of linear elasticity. Consequently, one prescribes

$$\lambda = \kappa_1\rho_0 A, \qquad \lambda y^{11} = \kappa_1\kappa_2\rho_0 I_2, \qquad \lambda y^{22} = \kappa_1\kappa_3\rho_0 I_1, \tag{12}$$

where κ_i are positive constants. The constants can be interpreted as correction factors in the sense of the shear coefficient in Timoshenko's beam theory, the coefficients κ and κ_1 in the Mindlin–Herrmann rod theory [26], and the coefficients α_3 and α_2–α_7 in Krishnaswamy

and Batra's works [23–25]. However, in contrast to these works, using equation (12) does not effect the static responses predicted by the rod theory. Prescriptions for κ_i will be discussed in section 5.

For completeness, an expression for the kinetic energy $\mathscr{T}$ of the model is recorded:

$$\mathscr{T} = \frac{\kappa_1}{2}\int_0^L \left(A\left(\frac{\partial u_3}{\partial t}\right)^2 + \kappa_2 I_2 \left(\frac{\partial \delta_{11}}{\partial t}\right)^2 + \kappa_3 I_1 \left(\frac{\partial \delta_{22}}{\partial t}\right)^2 \right) \rho_0 \, \mathrm{d}\xi. \tag{13}$$

This expression is obtained by simplifying the expression for the kinetic energy of the directed curve recorded by Naghdi [20] and using equations (12). It may be used in a standard manner to construct orthogonality relations for the eigenmodes.

3. FORMULATION OF THE FREE-VIBRATION PROBLEM

Motivated by the constitutive equations (9) and (10), it is convenient to define the displacement fields

$$\delta = \delta_{11} + \delta_{22}, \qquad \gamma = \delta_{11} - \delta_{22}. \tag{14}$$

Here, δ is twice the average lateral deformation while γ is the difference between the height-wise and width-wise deformations. Further, the dimensionless field U_3 and dimensionless variables b, s, and τ are introduced:

$$U_3 = \frac{u_3}{h}, \qquad b = \frac{h^2}{w^2}, \qquad s = \frac{\xi}{h}, \qquad \tau = t\sqrt{\frac{\alpha_3}{\lambda h^2}} = t\frac{c_d}{h\sqrt{\kappa_1}}, \tag{15}$$

where c_d is the dilational wave speed (in an unbounded medium of the three-dimensional theory of elasticity):

$$c_d = \sqrt{\frac{E}{\rho_0}\frac{(1-\nu)}{(1+\nu)(1-2\nu)}}. \tag{16}$$

From equations (6) and (14), the balance laws can be written in the form

$$\mathbf{x}'' + \mathbf{G}\mathbf{x}' + \mathbf{K}\mathbf{x} + \mathbf{F} = \mathbf{M}\ddot{\mathbf{x}}, \tag{17}$$

where

$$\mathbf{x} = \begin{bmatrix} U_3 \\ \delta \\ \gamma \end{bmatrix}, \quad \mathbf{F} = \begin{bmatrix} \dfrac{\lambda f_3 h}{\alpha_3} \\ \dfrac{\lambda l_{11} h^2}{\alpha_{10}} + \dfrac{\lambda l_{22} h^2}{\alpha_{11}} \\ \dfrac{\lambda l_{11} h^2}{\alpha_{10}} - \dfrac{\lambda l_{22} h^2}{\alpha_{11}} \end{bmatrix}, \quad \mathbf{G} = \begin{bmatrix} 0 & g(\nu) & 0 \\ -f(\nu)(1+b) & 0 & 0 \\ -f(\nu)(1-b) & 0 & 0 \end{bmatrix},$$

$$\mathbf{K} = \begin{bmatrix} 0 & 0 & 0 \\ 0 & -\dfrac{1+b}{2}\left(\dfrac{f(\nu)}{g(\nu)} + f(\nu)\right) & -\dfrac{1-b}{2}\left(\dfrac{f(\nu)}{g(\nu)} - f(\nu)\right) \\ 0 & -\dfrac{1-b}{2}\left(\dfrac{f(\nu)}{g(\nu)} + f(\nu)\right) & -\dfrac{1+b}{2}\left(\dfrac{f(\nu)}{g(\nu)} - f(\nu)\right) \end{bmatrix},$$

$$\mathbf{M} = \begin{bmatrix} 1 & 0 & 0 \\ 0 & \dfrac{1}{24}\dfrac{f(v)}{g(v)}(\kappa_2 + \kappa_3) & \dfrac{1}{24}\dfrac{f(v)}{g(v)}(\kappa_2 - \kappa_3) \\ 0 & \dfrac{1}{24}\dfrac{f(v)}{g(v)}(\kappa_2 - \kappa_3) & \dfrac{1}{24}\dfrac{f(v)}{g(v)}(\kappa_2 + \kappa_3) \end{bmatrix}, \tag{18}$$

and

$$f(v) = \frac{\alpha_7 h^2}{\alpha_{10}} = \frac{24v}{1-2v}, \quad g(v) = \frac{\alpha_7}{\alpha_3} = \frac{v}{1-v}. \tag{19}$$

In equation (17), $'$ indicates the partial derivative with respect to s, while the superposed dot indicates the partial derivative with respect to τ. For physically reasonable values of the Poisson ratio, $0 < v < 0{\cdot}5$, $g(v) \in (0, 1)$.

One now seeks harmonic solutions of equation (17), $\mathbf{x} = \mathbf{X}e^{i\Omega\tau}$, in the absence of applied body forces and surface tractions, $\mathbf{F} = \mathbf{0}$. For future purposes, it is convenient to define $U(s)$, $V(s)$, and $W(s)$:

$$\delta(s,\tau) = V(s)e^{i\Omega\tau}, \quad \gamma(s,\tau) = W(s)e^{i\Omega\tau}, \quad U_3(s,\tau) = U(s)e^{i\Omega\tau}. \tag{20}$$

Substituting equation (20) into equation (17) and setting $\mathbf{F} = \mathbf{0}$, one obtains the ordinary differential equations

$$\mathbf{X}'' + \mathbf{G}\mathbf{X}' + (\mathbf{K} + \Omega^2\mathbf{M})\mathbf{X} = \mathbf{0}. \tag{21}$$

For a given Ω, the solutions of equation (21) can be inferred by determining the eigenvalues β of the equilibrium $\mathbf{X} = \mathbf{0}$:

$$\det\begin{pmatrix} \beta\mathbf{I} & -\mathbf{I} \\ \mathbf{K} + \Omega^2\mathbf{M} & \beta\mathbf{I} + \mathbf{G} \end{pmatrix} = 0. \tag{22}$$

With some manipulations, this equation reduces to

$$m(\beta, \Omega) = 0, \tag{23}$$

where

$$m(\beta, \Omega) = \beta^6 + a_1\beta^4 + a_2\beta^2 + a_3 \tag{24}$$

and

$$\begin{aligned} a_1 &= (1+b)(g^2(v)-1)\frac{f(v)}{g(v)} + \left(1 + (\kappa_2+\kappa_3)\frac{f(v)}{12g(v)}\right)\Omega^2, \\ a_2 &= ((\kappa_2+\kappa_3)\Omega^2 - 12(1+b))\frac{f(v)\Omega^2}{12g(v)} + (2g(v)-3)bf^2(v) \\ &\quad + (\kappa_3 + b\kappa_2)\frac{f^2(v)\Omega^2}{12} + \frac{f^2(v)}{g^2(v)}\left(b - \frac{(\kappa_3 + b\kappa_2)\Omega^2}{12}\right) + \frac{\kappa_2\kappa_3 f^2(v)}{144g^2(v)}\Omega^4, \\ a_3 &= \left((1-g^2(v))b - (\kappa_2 + b\kappa_3)\frac{\Omega^2}{12} + \kappa_2\kappa_3\left(\frac{\Omega^2}{12}\right)^2\right)\frac{f^2(v)\Omega^2}{g^2(v)}. \end{aligned} \tag{25}$$

To discuss the eigenspectrum $\beta(\Omega)$, it is convenient to consider the cases $\beta = 0$. These arise when $\Omega^2 = 0$ and

$$\Omega^2 = \Omega_{1,2}^2 = \frac{6}{\kappa_2 \kappa_3}(\kappa_3 + b\kappa_2 \mp \sqrt{(\kappa_3 - b\kappa_2)^2 + 4b\kappa_2\kappa_3 g^2(\nu)}). \tag{26}$$

The case $\Omega = 0$ corresponds to the static solution—it is not considered here.

With the assistance of equation (26) and numerical explorations of the solutions of equation (23) for various values of ν, κ_2, κ_3, $b = h^2/w^2$, and Ω, five distinct cases arise. Each of these cases corresponds to a distinct spectrum of β:

Case I: $0 < \Omega < \Omega_1$, $\beta_{1,2} = \pm k_1$, $\beta_{3,4} = \pm k_2$, $\beta_{5,6} = \pm \mathrm{i}\mu_1$;
Case II: $\Omega = \Omega_1$; $\beta_{1,2} = \pm k_3$, $\beta_{3,4} = \pm i\mu_2$, $\beta_{5,6} = 0$;
Case III: $\Omega_1 < \Omega < \Omega_2$, $\beta_{1,2} = \pm k_4$, $\beta_{3,4} = \pm \mathrm{i}\mu_3$, $\beta_{5,6} = \pm \mathrm{i}\mu_4$;
Case IV: $\Omega = \Omega_2$, $\beta_{1,2} = \pm \mathrm{i}\mu_5$, $\beta_{3,4} = \pm \mathrm{i}\mu_6$, $\beta_{5,6} = 0$;
Case V: $\Omega > \Omega_2$, $\beta_{1,2} = \pm \mathrm{i}\mu_7$, $\beta_{3,4} = \pm \mathrm{i}\mu_8$, $\beta_{5,6} = \pm \mathrm{i}\mu_9$.

Here, $k_1, \ldots, k_4$ and $\mu_1, \ldots, \mu_9$ are real-valued functions of Ω, h/w, and ν. The cases where $\Omega = \Omega_{1,2}$ are similar to the thickness-shear mode observed in Timoshenko's beam theory (see references [29, 30] and references therein).

The general solutions of equation (17) for the five cases can be obtained in a standard manner. Each set of solutions involves six constants $A_1, \ldots, A_6$.[§] Postponing the case $b = 1$, $b \neq 1$ is presently assumed. First, for Cases I, III, and V,

$$U(s) = \sum_{K=1}^{6} A_K \mathrm{e}^{\beta_K s}, \quad V(s) = \sum_{K=1}^{6} f_1(\beta_K) A_K \mathrm{e}^{\beta_K s},$$

$$W(s) = \sum_{K=1}^{6} f_2(\beta_K) A_K \mathrm{e}^{\beta_K s}. \tag{27}$$

For the remaining two cases,

$$U(s) = \sum_{K=1}^{4} A_K \mathrm{e}^{\beta_K s} - \frac{g(\nu)}{\Omega_\alpha^2} A_5,$$

$$V(s) = \sum_{K=1}^{4} f_1(\beta_K) A_K \mathrm{e}^{\beta_K s} + A_5 s + A_6,$$

$$W(s) = \sum_{K=1}^{4} f_2(\beta_K) A_K \mathrm{e}^{\beta_K s} + \left(\frac{(\kappa_2 + \kappa_3)\Omega_\alpha^2/24g(\nu) - (1 + b/2)(1/g(\nu) + 1)}{(1 - b/2)(1/g(\nu) - 1) - (\kappa_2 - \kappa_3)\Omega_\alpha^2/24g(\nu)} \right)(A_5 s + A_6), \tag{28}$$

where $\alpha = 1$ for Case II and $\alpha = 2$ for Case IV. In equations (27) and (28), the following functions were used:

$$f_1(\beta) = -\frac{\beta^2 + \Omega^2}{g(\nu)\beta},$$

$$f_2(\beta) = \frac{(\beta^2/f(\nu) - (1 + b/2)(1/g(\nu) + 1\ ) + (\kappa_2 + \kappa_3)\Omega^2/24g(\nu))f_1(\beta) - (1 + b)\beta}{(1 - b/2)(1/g(\nu) - 1) - 1/24g(\nu)(\kappa_2 - \kappa_3)\Omega^2}. \tag{29}$$

[§]These solutions could be expressed in terms of trigonometric and hyperbolic functions. However, in the interests of brevity, a notation involving exponential functions is used.

For Cases I, III, and V, five of the six constants $A_1, \ldots, A_6$ and Ω are determined using the boundary conditions in a standard manner. However, for Cases II and IV, the boundary conditions are used to determine five of these constants and establish an existence criterion for a solution of the form (28).

4. A ROD WITH A SQUARE CROSS-SECTION

The free-vibration problem when the rod has a square cross-section, $h = w$, is considerably simpler than the rectangular case. For this rod it can be argued on the basis of symmetry that $\kappa_2 = \kappa_3$. With this in mind, the ordinary differential equations (21) decouple into two sets:

$$U'' + g(v)V' + \Omega^2 U = 0,$$

$$V'' - 2f(v)U' - \frac{f(v)}{g(v)}\left(1 + g(v) - \frac{\Omega^2\kappa_2}{12}\right)V = 0, \tag{30}$$

and

$$W'' - \frac{f(v)}{g(v)}\left(1 - g(v) - \frac{\Omega^2\kappa_2}{12}\right)W = 0. \tag{31}$$

For this case, the expressions for the frequencies $\Omega_{1,2}$ simplify to

$$\Omega_1^2 = \frac{12}{\kappa_2}(1 - g(v)) = \frac{12(1-2v)}{\kappa_2(1-v)}, \quad \Omega_2^2 = \frac{12}{\kappa_2}(1 + g(v)) = \frac{12}{\kappa_2(1-v)}. \tag{32}$$

These results were obtained from equation (26).

It is opportune to remark that equations (30) are similar to the equations considered by Mindlin and Herrmann [26] and Krishnaswamy and Batra [23] for a circular rod. Although these authors assume symmetric vibrations (i.e., $\delta_{11} = \delta_{22}$), it will become apparent that in many cases the asymmetric vibrations decouple from the U–V vibrations and may be calculated independently. In addition, there are several evident similarities between the results for the symmetric lateral vibrations when the cross-section is square and when it is circular.

Following the procedure discussed in section 3, one solves for $U(s)$ and $V(s)$ to find for Cases I, II, III, and V that

$$U(s) = \sum_{K=1}^{4} A_K e^{\beta_K s}, \quad V(s) = -\sum_{K=1}^{4} \frac{\beta^2 + \Omega^2}{g(v)\beta} A_K e^{\beta_K s}, \tag{33}$$

where $\beta_{1,2,3,4}$ are the solutions of

$$\beta^4 + \left(2f(v)g(v) + \frac{f(v)\kappa_2}{12g(v)}(\Omega^2 - \Omega_2^2) + \Omega^2\right)\beta^2 + \frac{f(v)\kappa_2\Omega^2}{12g(v)}(\Omega^2 - \Omega_2^2) = 0. \tag{34}$$

For Case IV, $\Omega = \Omega_2 = \sqrt{\frac{12}{\kappa_2}(1 + g(v))}$, and the general solution is

$$U(s) = A_1\cos(\chi s) + A_2\sin(\chi s) - \frac{g(v)}{\Omega_2^2}A_3,$$

$$V(s) = \frac{-\chi^2 + \Omega_2^2}{g(v)\chi}(A_2\cos(\chi s) - A_1\sin(\chi s)) + A_3 s + A_4. \tag{35}$$

Here,

$$\chi = \sqrt{2f(v)g(v) + \Omega_2^2}, \tag{36}$$

is the imaginary part of one of the non-zero roots β of equation (34).

One next solves for W, to find, for Cases I, III, IV, and V, that

$$\delta_{11} - \delta_{22} = (A_5 e^{\beta_5 s} + A_6 e^{\beta_6 s}) e^{i\Omega\tau}, \tag{37}$$

where A_5 and A_6 are determined by the boundary and initial conditions, and

$$\beta_{5,6} = \pm \sqrt{\frac{f(v)\kappa_2}{12g(v)}(\Omega_1^2 - \Omega^2)}. \tag{38}$$

When $\Omega = \Omega_1 = \sqrt{\dfrac{12}{\kappa_2}(1 - g(v))}$, $\beta_{5,6} = 0$, and, as a result,

$$\delta_{11} - \delta_{22} = (A_5 s + A_6) e^{i\Omega_1\tau} \tag{39}$$

is the solution of equation (31) for Case II. Here, A_5 and A_6 are constants.

It should be noted that the degenerate Case II pertains only to the vibrations associated with $\delta_{11} - \delta_{22}$, while Case IV only pertains to the vibrations associated with $\delta_{11} + \delta_{22}$ and u_3. Further, if the boundary conditions permit, Ω for the latter modes is determined from the frequency equation for equations (30), while Ω for the modes associated with $\delta_{11} - \delta_{22}$ is determined independently from the frequency equation for equation (31). A specific example shall presently be discussed to illustrate these comments.

5. PRESCRIPTIONS FOR κ_1, κ_2, AND κ_3

The general solutions discussed in the previous section depend on the three parameters κ_i. Among other issues, wave propagation in an infinitely long parallelepiped is examined in order to specify κ_i.

The present interest is in solutions of the form

$$\delta(s,\tau) = B_1 e^{ik(s - c\tau)}, \quad \gamma(s,\tau) = B_2 e^{ik(s - c\tau)}, \quad U_3(s,\tau) = B_3 e^{ik(s - c\tau)}. \tag{40}$$

Here, B_i are constants, k is a dimensionless wavenumber, and c is a dimensionless wave speed. Substituting equations (40) into equation (17), a set of three coupled linear equations for B_i are obtained. For the existence of non-trivial solutions, it is necessary that c and k satisfy the characteristic equation associated with these equations. The characteristic equation is (cf. equation (23))

$$m(\beta = ik, \Omega = -kc) = 0. \tag{41}$$

The three solutions $c_i(k)$ of this equation define the dispersion relations for the rod (cf. Figure 3).[¶] One should also note that the (dimensioned) wave speed $\bar{c} = c_d/\sqrt{\kappa_1}\, c$.

Examining the solutions of equation (41) one notices that there are three branches (I, II, and III). The extreme limits of these branches are important. First, for short wavelengths,

[¶]This figure, along with Figures 4, 5, and 7–10 were obtained with the assistance of the contour plotting algorithm of the symbolic manipulation package *Mathematica* [35].

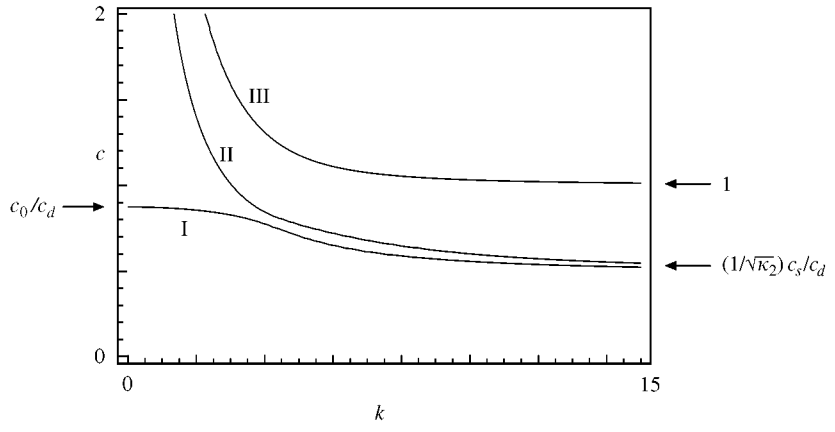

Figure 3. Dimensionless wave velocities of an infinite rod with a rectangular cross-section $h/w = 1{\cdot}5$ as a function of the dimensionless wavenumber k. For this figure, $\nu = 0{\cdot}290$, $\kappa_2 = \kappa_3 = 12/\pi^2$.

the limiting wave velocities are

$$\lim_{k\to\infty} c^2 = \frac{1}{\kappa_2}\frac{c_s^2}{c_d^2}, \quad \frac{1}{\kappa_3}\frac{c_s^2}{c_d^2}, \ 1, \tag{42}$$

where $c_s = \sqrt{E/2\rho_0(1+\nu)}$ is the shear wave speed. The limiting speeds of Branches I and III are given by the minimum and maximum, respectively, of these three values. At the other extreme,

$$\lim_{k\to 0} c_1^2 = \frac{c_0^2}{c_d^2}, \quad \infty, \quad \infty, \tag{43}$$

where $c_0 = \sqrt{E/\rho_0}$ is the bar wave speed. Here, c_0/c_d is the limiting wave speed of Branch I. For a rod with a square cross-section, Branches I and III are associated with the u–δ displacements while Branch II is associated with the γ displacements. When the rod has a rectangular cross-section, the wave propagations of these two sets of displacements become coupled.

The aforementioned limiting wave velocities can be used to prescribe κ_i as follows. First, following Chree's result in reference [3] for rods of arbitrary cross-section, κ_1 is chosen such that the (finite) short wavelength limit of c coincides with the bar wave speed. Consequently,

$$\kappa_1 = 1. \tag{44}$$

The selection of κ_2 and κ_3 is not as clear-cut. These coefficients should be obtained by examining the wave speeds of extensional waves in a rectangular plate. However, no exact solution from three-dimensional linear elasticity is available for this case.‖

For the case of a rod with a square cross-section, the exact solution, from three-dimensional linear elasticity, for vibrations of a parallelepiped where $u_3 = 0$ is considered.†† The (dimensionless) frequency associated with this solution is denoted by

‖As Green [2] has pointed out, most of the approximate solutions for wave propagation in infinite rods of non-circular cross-sections are not valid in the short wavelength limit.

††The solution is due to Lamé [7]. It is discussed in references [8–10, 15]. In the notation of reference [15], the solution is $u_1 = a_1 \sin(\omega t)\sin(p_1^* x_1)\cos(p_1^* x_2)$ and $u_2 = -a_1 \sin(\omega t)\cos(p_1^* x_1)\sin(p_1^* x_2)$, where $\cos(p_1^* h/2) = 0$.

Ω_p where

$$\Omega_p = \frac{\sqrt{2}\pi c_s}{c_d}. \tag{45}$$

The counterpart of this exact solution in the rod theory of interest is assumed to correspond to a motion where $U = V = 0$ and W is non-zero. This solution can be obtained from equations (35) and (39) by setting $A_1, \ldots, A_5 = 0$. Following Mindlin and Deresiewicz [32] and Krishnaswamy and Batra [24], one prescribes κ_2 and κ_3 in order to match two frequencies: $\Omega_P = \Omega_1$. Noting that $\Omega_1 = \sqrt{24/\kappa_2}\,(c_s/c_d)$, this results in the prescription

$$\kappa_2 = \kappa_3 = \frac{12}{\pi^2} \approx 1{\cdot}21585. \tag{46}$$

Since suitable exact solutions from the three-dimensional theory of linear elasticity do not presently appear to be available when $h \neq w$, the conservative prescription (46) is also adopted for this case.‡‡

6. VIBRATIONS OF A FREE–FREE ROD

To illustrate the solutions of the vibrating rod model, consider the case of a free–free rod which has rectangular cross-sections ($b \neq 1$). For this rod, the boundary conditions are

$$U'(s=0) = -g(v)V(s=0), \quad U'\left(s=\frac{L}{h}\right) = -g(v)V\left(s=\frac{L}{h}\right),$$

$$V'(s=0) = 0, \quad V'\left(s=\frac{L}{h}\right) = 0, \quad W'(s=0) = 0, \quad W'\left(s=\frac{L}{h}\right) = 0. \tag{47}$$

To formulate these conditions, equations (8), (9), (10), (15), and (20) were used.

Using the boundary conditions and equations (27) and (28), the following equation is formed:

$$\mathscr{D}\mathscr{A} = \mathbf{0}, \tag{48}$$

where $\mathscr{A}$ is the column vector $[A_1, \ldots, A_6]$ and $\mathscr{D}$ is a six-by-six matrix. The elements D_{IK} of this matrix are, for Cases I, III, and V,

$$D_{1K} = -\frac{\Omega^2}{\beta_K}, \quad D_{2K} = -\frac{\Omega^2}{\beta_K}\,\mathrm{e}^{(\beta_K L/h)}, \quad D_{3K} = \frac{\beta_K^2 + \Omega^2}{g(v)},$$

$$D_{4K} = \frac{\beta_K^2 + \Omega^2}{g(v)}\mathrm{e}^{(\beta_K L/h)}, \quad D_{5K} = \beta_K f_2(\beta_K), \quad D_{6K} = \beta_K f_2(\beta_K)\mathrm{e}^{(\beta_K L/h)}, \tag{49}$$

where $K = 1, \ldots, 6$. For Cases II and IV, the components are

$$D_{1K} = -\frac{\Omega_\alpha^2}{\beta_K}, \quad D_{2K} = -\frac{\Omega_\alpha^2}{\beta_K}\,\mathrm{e}^{(\beta_K L/h)}, \quad D_{3K} = \frac{\beta_K^2 + \Omega_\alpha^2}{g(v)},$$

$$D_{15} = 0, \quad D_{16} = g(v), \quad D_{25} = g(v)\frac{L}{h}, \quad D_{26} = g(v),$$

$$D_{35} = 1, \quad D_{36} = 0, \quad D_{45} = 1, \quad D_{46} = 0,$$

‡‡An alternative prescription might be to parallel the developments for the rods with a square cross-section, but use a finite-element analysis for a given parallelepiped to find modes of vibration where $u_3 = 0$. The two lowest frequencies of these modes could be used to prescribe κ_2 and κ_3. However, this approach is not pursued here.

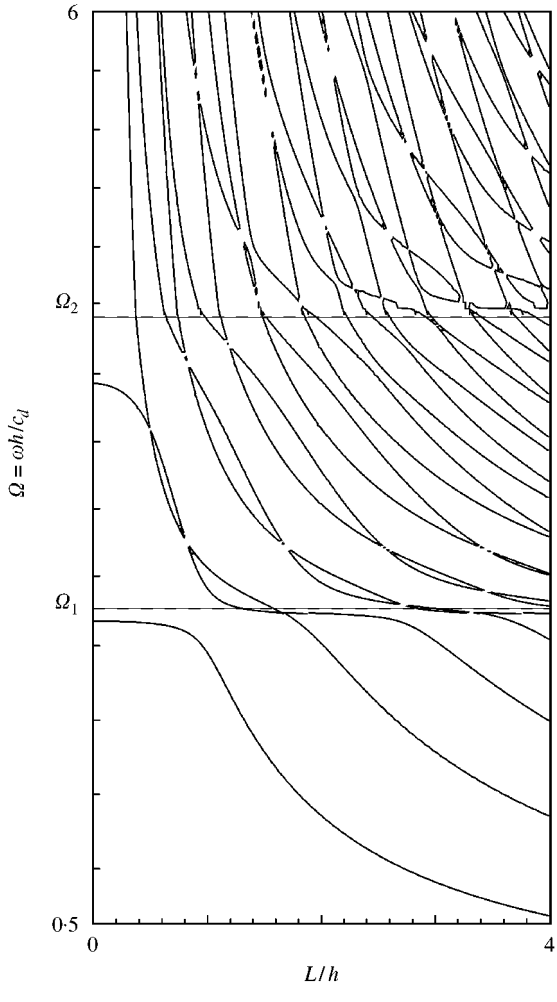

Figure 4. Dimensionless natural frequencies for a free–free rod with a rectangular cross-section as a function of the rod's slenderness ratio L/h. For this figure, $h/w = 1{\cdot}5$, $\nu = 0{\cdot}290$, $\kappa_1 = 1$, $\kappa_2 = \kappa_3 = 12/\pi^2$, and, consequently, $\Omega_1 = 2{\cdot}72031$ and $\Omega_2 = 4{\cdot}96751$.

$$D_{4K} = \frac{\beta_K^2 + \Omega_\alpha^2}{g(\nu)} e^{(\beta_K L/h)}, \quad D_{5K} = \beta_K f_2(\beta_K), \quad D_{6K} = \beta_K f_2(\beta_K)\, \mathrm{e}^{(\beta_K L/h)},$$

$$D_{55} = D_{65} = \frac{(\kappa_2 + \kappa_3)\Omega_\alpha^2/24g(\nu) - 1 + b/2(1/g(\nu) + 1)}{1 - b/2(1/g(\nu) - 1) - (\kappa_2 - \kappa_3)\Omega_\alpha^2/24g(\nu)}, \quad D_{56} = D_{66} = 0, \tag{50}$$

where $K = 1, \ldots, 4$, $\alpha = 1$ for Case II, and $\alpha = 2$ for Case IV.

The equation $\det(\mathscr{D}) = 0$ is the frequency equation. For Cases I, III, and V, this equation determines Ω.[§§] Numerical results for Ω as a function of the slenderness ratio L/h are shown in Figure 4. As the slenderless ratio increases, the frequency equation becomes increasingly ill-conditioned.[¶¶] Consequently, the range of L/h in Figure 4 is limited. The frequency curves

[§§]In the interests of brevity, the precise forms of the frequency equations for these cases are not presented here.

[¶¶]This ill-conditioning arises because the frequency equation contains hyperbolic and trigonometric functions. As the slenderness ratio increases, the terms involving the hyperbolic functions dominate the frequency equation and it becomes increasing difficult to solve the equation.

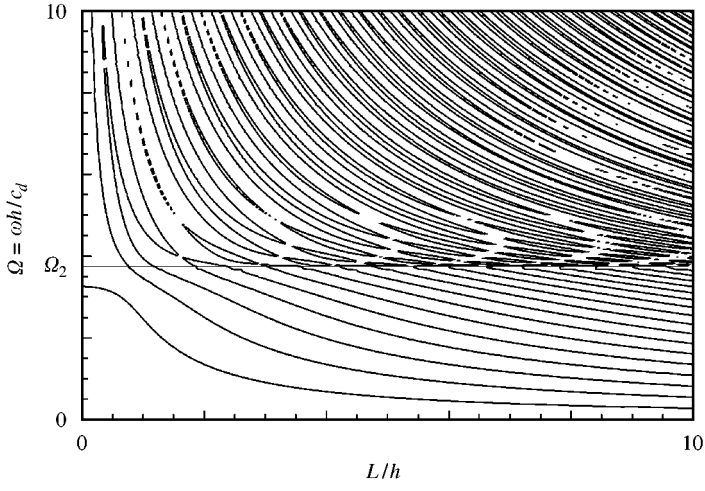

Figure 5. The dimensionless natural frequencies Ω for a free–free rod with a square cross-section as a function of the slenderness ratio L/h. For this figure, $\nu = 0{\cdot}290$, $\kappa_1 = 1$, $\kappa_2 = \kappa_3 = 12/\pi^2$, and, consequently, $\Omega_2 = 3{\cdot}72838$. The frequency curves displayed in this figure correspond to the modes $U(s)$ and $V(s)$.

in this figure can be compared to those predicted by the wave equation. For the wave equation (1), the corresponding frequency equation is

$$\sin\left(\frac{\Omega c_d}{c_0}\frac{L}{h}\right) = 0. \tag{51}$$

The solutions Ω of equation (51) provide good approximations to the first natural frequencies shown in Figure 4 for values of $L/h > 1$, and to the second natural frequency for $\Omega < \Omega_1$ and $L/h > 2{\cdot}5$. However, as is to be expected, the higher the Ω, the poorer the approximation (51) provides.

For Cases II and IV, the analysis used in reference [30] is followed. Specifically, Ω is known and $\det(\mathscr{D}) = 0$ is used to determine the combinations of geometric and material properties of the rod which support the modes (28). Referring to Figure 4, one can see that the intersection of the frequency curves $\Omega(L/h)$ and the lines $\Omega = \Omega_1$ and Ω_2 occurs at discrete values of the slenderness ratio. These values correspond to those that would be obtained from the equation $\det(\mathscr{D}) = 0$. For Cases II and IV, the null vectors of $\mathscr{D}$ determine the eigenmodes.

It would be desirable to compare the results of this section to predictions from the three-dimensional theory of elasticity. However, no published results on the vibrational frequencies of free–free parallelepipeds where $h \neq w$ appear to be available.

7. A FREE–FREE ROD WITH SQUARE CROSS-SECTIONS

To facilitate comparisons with other researches and because of its design importance, the case of a rod with a square cross-section and free–free boundary conditions is considered. For this rod, the boundary conditions are again given by equations (47). It should be clear that these boundary conditions preserve the decoupling of U and V from W. In the discussion, the modes associated with U and V are addressed first.

As shown in Figure 5, the natural frequencies as functions of L/h are calculated by first constructing the frequency equations associated with the boundary conditions. The details

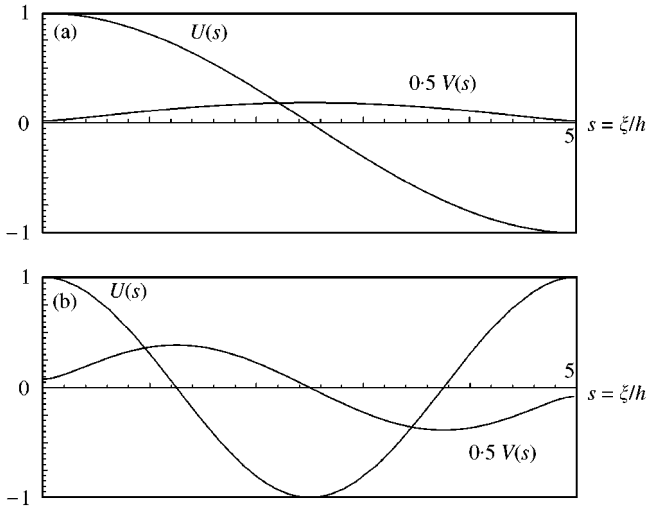

Figure 6. The first (a) and second (b) modes for a free–free rod with a square cross-section, $\nu = 0{\cdot}290$, $\kappa_1 = 1$, $\kappa_2 = \kappa_3 = 12/\pi^2$, and a slenderness ratio $L/h = 5$. For this rod, the first natural frequency is $\Omega = 0{\cdot}547527$, and the second is $\Omega = 1{\cdot}0866044$. For convenience the amplitude of the mode shape is chosen such that $U(0) = 1$. In addition, $V(s)/2$ are displayed because they correspond to the lateral deformation of the rod.

can be easily inferred from the developments of section 6. As is evident from Figure 5, the frequencies associated with the vibrations of $\delta_{11} + \delta_{22}$ and u_3 can be divided into two regions, dependent on whether the natural frequency is greater than or less than Ω_2. In the lower frequency regime, the modes are composed of hyperbolic and trigonometric terms—examples of which are shown in Figure 6. When $\Omega > \Omega_2$, these modes only contain trigonometric terms.

For a given ν, only certain discrete values of L/h support solutions of the form (35) where $\Omega = \Omega_2$. To find these points, one follows reference [30] and calculates the matrix $\mathscr{D}$:

$$\mathscr{D} = \begin{bmatrix} 0 & \dfrac{\Omega_2^2}{\chi} & 0 & g(\nu) \\ -\dfrac{\Omega_2^2}{\chi}\sin\left(\dfrac{\chi L}{h}\right) & \dfrac{\Omega_2^2}{\chi}\cos\left(\dfrac{\chi L}{h}\right) & \dfrac{g(\nu)L}{h} & g(\nu) \\ 2f(\nu) & 0 & 1 & 0 \\ 2f(\nu)\cos\left(\dfrac{\chi L}{h}\right) & 2f(\nu)\sin\left(\dfrac{\chi L}{h}\right) & 1 & 0 \end{bmatrix}. \tag{52}$$

The determinant of this matrix is zero if, and only if,

$$\tan\left(\frac{\chi L}{h}\right) + \frac{\chi f(\nu) g(\nu)}{12(1 + g(\nu))}\left(\frac{L}{h}\right) = 0. \tag{53}$$

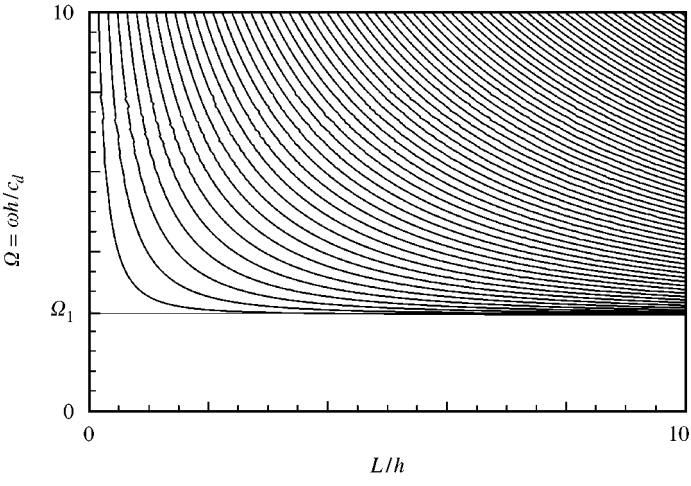

Figure 7. The dimensionless natural frequencies Ω associated with the asymmetric lateral vibrations of a free–free rod with a square cross-section as a function of the slenderness ratio L/h. For this figure, $\nu = 0{\cdot}290$, $\kappa_1 = 1$, $\kappa_2 = \kappa_3 = 12/\pi^2$, and, consequently, $\Omega_1 = 2{\cdot}41627$. The frequency curves displayed in this figure correspond to the mode $W(s)$. It should be noted that these frequencies can never be smaller than Ω_1.

For a given ν, this equation determines L/h which supports the natural frequency Ω_2. For completeness, the corresponding eigenmode is also recorded:

$$U(s) = A_1\left(\cos(\chi s) + \tan\left(\frac{\chi L}{2h}\right)\sin(\chi s) + \frac{2f(\nu)g(\nu)}{\Omega_2^2}\right),$$

$$V(s) = A_1\left(\frac{2f(\nu)}{\chi}\right)\left(\sin(\chi s) - 2\chi s - \tan\left(\frac{\chi L}{2h}\right)\cos(\chi s)\right)$$

$$- A_1\left(\frac{\Omega_2^2}{g(\nu)\chi}\right)\tan\left(\frac{\chi L}{2h}\right). \tag{54}$$

Here, the constant A_1 is determined from the initial conditions using equations (13).

Turning to the solutions for δ_{11}–δ_{22}, one finds that these solutions are not supported in a free–free rod when $\Omega < \Omega_1$ (cf. equation (37)). From equation (39) and the boundary conditions, one finds that the eigenmode when $\Omega = \Omega_1$ is $W(s) = A_6$. This mode can be excited in all square rods. For higher frequencies, the eigenmode is

$$W(s) = A_5\cos(\sigma s) + A_6\sin(\sigma s), \tag{55}$$

where $\sigma^2 = f(\nu)\kappa_2/12g(\nu)(\Omega^2 - \Omega_1^2)$ (cf. equation (38)). Further, Ω is determined from the characteristic equation

$$\sin\left(\frac{L}{h}\sqrt{\frac{f(\nu)\kappa_2}{12g(\nu)}(\Omega^2 - \Omega_1^2)}\right) = 0. \tag{56}$$

The solutions of this equation as functions of the slenderness ratio L/h are displayed in Figure 7.

The results of the model's predictions can be compared to the work of Hutchinson and Zillmer [11]. These authors used the three-dimensional theory of linear elasticity and consider solutions of these equations which are sums of products of trigonometric functions.

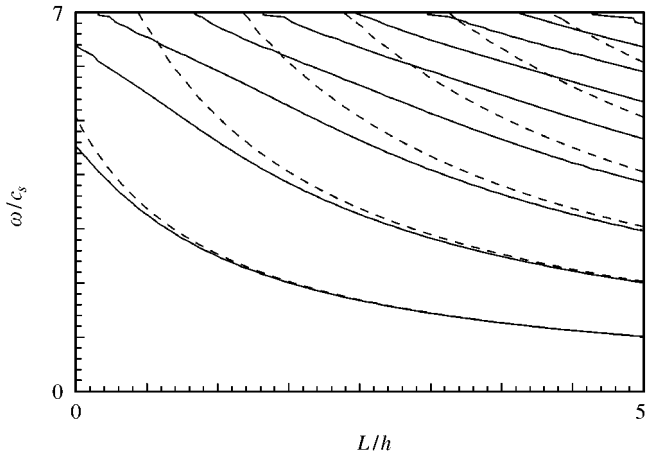

Figure 8. Comparison of the natural frequencies ω/c_s associated with the symmetric lateral vibrations of a free–free rod with a square cross-section with those predicted using the wave equation. The solid lines in this figure correspond to the U–V vibrations where $\Omega < \Omega_2$, while the dashed lines correspond to the first six natural frequencies predicted by the wave equation. For this figure, $\nu = 0{\cdot}300$, $h = w = 1{\cdot}0$, $\kappa_1 = 1$, and $\kappa_2 = \kappa_3 = 12/\pi^2$.

As a result, their solutions are not equivalent to those considered in this paper. However, the asymptotic behavior of the frequencies of these solutions can be approximated by the corresponding frequencies for the wave equation (cf. equation (51)). In addition, these authors present results for a parallelepiped where $h = w = 0{\cdot}5$, $\nu = 0{\cdot}3$ and L varies.[‖‖] To facilitate the comparison, results for the U–V vibrations of the parallelepiped are shown in Figure 8. In this figure, the dotted lines represent the corresponding results predicted by the wave equation (cf. equations (1) and (51). Comparing the results of Figure 8 to those presented in Figures 4 and 5 of reference [11], it is evident that the frequencies of the modes can be approximated using equation (51) provided that L/h is sufficiently large. It is also evident from Figure 8, that the behavior of frequency spectra for the U–V modes as L/h gets smaller, is not the same as those for the modes discussed in reference [11].

Hutinchson and Zillmer [11] do not present results for $L/h < 1$. It is to be expected, however, that the behavior of the frequency spectra should be qualitatively similar to those for a circular cylinder. Rumerman and Raynor [36], using the three-dimensional theory of elasticity, have presented results for the cylinder. Krishnaswamy and Batra [23] and McNiven and Perry [37] examined the cylinder using rod theories. Referring to Figure 5, the frequency spectrum results for the lowest mode agrees rather well with references [23, 36, 37]. As $L/h \to 0$, $\Omega \to \approx 3{\cdot}3$. This frequency is known as the plate frequency. For a circular disk of radius $0{\cdot}5h$ and $\nu = 0{\cdot}29$, the plate frequency is $\Omega \approx 3{\cdot}7$ (cf. p. 498 of reference [1]). However, for the second mode, it is to be anticipated that the frequency should tend to zero as $L/h \to 0$. Clearly, this is not the case. A related discrepency arises in the results of McNiven and Perry [37] and Krishnaswamy and Batra [23].

8. A FIXED–FREE ROD

In order to compare the frequency spectra predicted by the model with the results of other researchers who used the three-dimensional theory of linear elasticity, it is convenient

[‖‖] In the notation of reference [11], $2b = L$, $2c = h$, and $2a = w$. Their pertinant results are supposed to be presented in Figures 4 and 5 of reference [11]. However, as noted in footnote 4 of Rubin [15], the plots for Figures 6 and 7 were juxtaposed with those for Figures 4 and 5, respectively.

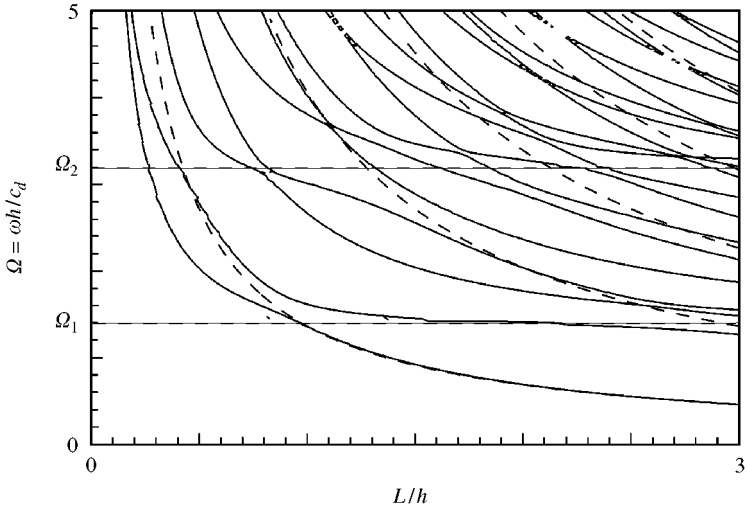

Figure 9. The dimensionless natural frequencies Ω associated with the vibrations of a cantilevered rod with a rectangular cross-section as a function of the slenderness ratio L/h. For this figure, $\nu = 0{\cdot}30$, $h/w = 0{\cdot}5$, $\kappa_1 = 1$, $\kappa_2 = \kappa_3 = 12/\pi^2$, and, consequently, $\Omega_1 = 1{\cdot}38049$ and $\Omega_2 = 3{\cdot}22974$. The dashed lines in the figure correspond to the frequencies predicted by the wave equation (1).

to consider the case of the cantilevered rod. Here, the boundary conditions are

$$U(s=0)=0, \quad V(s=0)=0, \quad W(s=0)=0,$$

$$U'\left(s=\frac{L}{h}\right) = -g(\nu)V\left(s=\frac{L}{h}\right), \quad V'\left(s=\frac{L}{h}\right)=0, \quad W'\left(s=\frac{L}{h}\right)=0. \tag{57}$$

To formulate these conditions, equations (7)–(10), (15), and (20) were used. Using the boundary conditions and equations (27) and (28), a frequency equation is formed and the frequency spectra and eigenmodes can be calculated. Because the results are similar to those discussed in the previous two sections, details of the calculations are omitted and summaries of the results are presented.

The frequency spectra predicted by the model are shown in Figure 9 for the case of a particular rectangular cross-section. In this figure, the corresponding frequencies predicted by the wave equation (1) are also shown. It should be noted that the first mode frequency predicted by the wave equation agrees with that predicted by the model for $L/h > 1$. For the higher modes, this agreement occurs at far higher values of L/h as expected. The corresponding results for the case of a square cross-section are shown in Figure 10. In this case, the U–V modes decouple from the W modes. Furthermore, the latter modes only exist when $\Omega > \Omega_1$. It is interesting to note that although the frequency spectra for the U–V modes asymptote to those predicted by the wave equation as the slenderness ratio is increased, no such correspondance exists between frequency curves for the W modes and those predicted by the wave equation. Examples of the eigenmodes for a particular cantilevered rod with a rectangular cross-section can be found in Figures 6.6 and 6.7 of Turcotte [22].

The selection of parameters for Figures 9 and 10 was motivated by the results of Leissa and Zhang [13]. These authors considered vibrations of a cantilevered parallelepiped. By constructing approximate solutions to the three-dimensional theory of elasticity for this

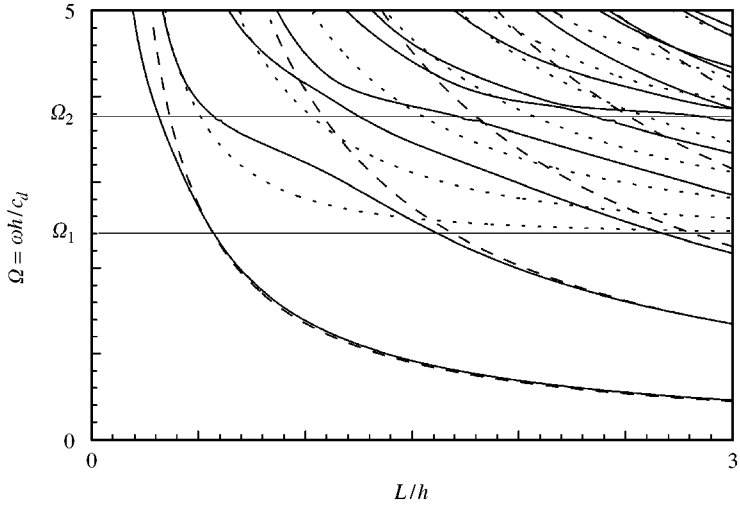

Figure 10. The dimensionless natural frequencies Ω associated with the vibrations of a cantilevered rod with a square cross-section as a function of the slenderness ratio L/h. For this figure, $\nu = 0{\cdot}30$, $\kappa_1 = 1$, $\kappa_2 = \kappa_3 = 12/\pi^2$, and, consequently, $\Omega_1 = 2{\cdot}37482$ and $\Omega_2 = 3{\cdot}75492$. The solid lines correspond to the U–V modes, the light dashed (·····) lines correspond to the W modes, and the dashed lines (- - - - -) in the figure correspond to the frequencies predicted by the wave equation (1).

TABLE 1

Comparison of natural frequencies Ω for cantilivered parallelepipeds

Dimensions	Frequencies			
	Mode 1	Mode 2	Mode 3	Mode 4
$\frac{L}{h} = \frac{h}{w} = 1{\cdot}0$	1·39 (1·38)‡	2·8†,‡ (2·22)	3·23 (2·51)	3·86† (2·63)
$\frac{L}{h} = 2{\cdot}0, \frac{h}{w} = 1{\cdot}0$	0·688 (0·69)	1·99 (1·97)	2·49† (2·18)	2·82† (2·37)
$\frac{L}{h} = 2{\cdot}0, \frac{h}{w} = 0{\cdot}5$	0·690 (0·690)	1·40 (1·21)	1·77 (1·38)	2·03 (1·88)
$\frac{L}{h} = 0{\cdot}5, \frac{h}{w} = 1{\cdot}0$	2·71 (2·53)	3·86† (2·63)	3·94 (3·10)	5·78 (3·18)
$\frac{L}{h} = 1{\cdot}0, \frac{h}{w} = 0{\cdot}5$	1·35 (1·32)	1·61 (1·45)	2·65 (1·75)	3·01 (2·43)

†Correspond to W modes for the cases $w/h = 1$.
‡Results in parenthesis are from Table 2 of reference [13].

problem, they calculated the frequency spectra for various configurations. In Table 1, some of Leissa and Zhang's results are presented along with the corresponding results predicted by the model used in this paper. It is evident from the table that the natural frequency for the first mode agrees rather well with the results of reference [13]. Indeed, for the cases considered in Table 1, $L/h = 0{\cdot}5$, $L/h = 1{\cdot}0$, and $L/h = 2{\cdot}0$, the wave equation predicts a first

natural frequencies of $\Omega = 2{\cdot}71$, $1{\cdot}44$, and $0{\cdot}677$, respectively. However, the discrepencies between Leissa and Zhang's results and the frequencies predicted by the model used in the present paper become increasingly larger for the higher modes. This matter can be partially explained when one considers the nature of the displacement fields considered in reference [13] and the present paper (cf. equations (3) and (4)). Specifically, the model discussed in section 2 assumes that the lateral displacement varies linearly through the cross-section, whereas the displacement field used in reference [13] allows trigonometric and hyperbolic variations.

9. CLOSING REMARKS

With the assistance of equations (3), (4), and (14), it can be shown that the displacement field $\mathbf{u}^*$ of a point of the parallelepiped examined in this paper is

$$\mathbf{u}^*(x_i, t) = \frac{x_1}{2}\left(V\left(\frac{x_3}{h}\right) + W\left(\frac{x_3}{h}\right)\right)e^{i\omega t}\mathbf{E}_1 + \frac{x_2}{2}\left(V\left(\frac{x_3}{h}\right) - W\left(\frac{x_3}{h}\right)\right)e^{i\omega t}\mathbf{E}_2 + hU\left(\frac{x_3}{h}\right)e^{i\omega t}\mathbf{E}_3. \tag{58}$$

In discussions of the Poisson effect, it is usual to consider a bar in a state of uniaxial tension (cf. section 112 of reference [1]). In this case, the lateral displacement fields, u_1 and u_2, are related to the longitudinal displacement field $u_3 = \varepsilon x_3$:

$$u_1 = -\nu\varepsilon x_1, \quad u_2 = -\nu\varepsilon x_2, \tag{59}$$

where ε is a constant. Clearly, the displacement field (58) is not of this form.[†††] When one realizes that the modes of vibration of the rod-like body discussed in this paper do not correspond to the body in a state of uniaxial tension, then this conclusion becomes evident.

It is of interest to examine how the modes discussed in this paper can be excited using tractions applied to its lateral surface. It shall be assumed that the ends $x_3 = 0$ and L are traction-free. To examine this issue, consider the static problem of deforming a rod-like body such that its static displacement field $\mathbf{u}(x_i) = \mathbf{u}^*(x_i, t)\,e^{-i\omega t}$. Using equations (3), (4), (6), (17), and (58), this static solution satisfies the balance laws (6) if

$$\lambda f_3 = \omega^2\lambda U\left(\frac{x_3}{h}\right), \quad \lambda l_{11} = \frac{\omega^2\lambda y^{11}}{2}\left(V\left(\frac{x_3}{h}\right) + W\left(\frac{x_3}{h}\right)\right),$$
$$\lambda l_{22} = \frac{\omega^2\lambda y^{22}}{2}\left(W\left(\frac{x_3}{h}\right) - V\left(\frac{x_3}{h}\right)\right). \tag{60}$$

Prescriptions for $\lambda\mathbf{f}$, $\lambda\mathbf{l}^1$, and $\lambda\mathbf{l}^2$ are presented in references [19, 20]:

$$\lambda\mathbf{f} = \oint_c \mathbf{t}\,ds, \quad \lambda\mathbf{l}^1 = \oint_c \mathbf{t}x_1\,ds, \quad \lambda\mathbf{l}^2 = \oint_c \mathbf{t}x_2\,ds, \tag{61}$$

where s is the arc-length parameter of the curve c and $\mathbf{t}$ is the traction vector. As shown in Figure 2, c is the bounding curve of a cross-section. Combining equation (60) with equation

[†††] If one considers static solutions of the balance laws for the directed curve which are appropriate to the uniaxial tension case, then a solution of the form (59) will be obtained (cf. equations (9.11)–(9.15) of reference [18]): $\delta_{11} = \delta_{22} = -\nu(\partial u_3/\partial\xi)$.

(61), three equations for the components $t_i = \mathbf{t} \cdot \mathbf{E}_i$ of $\mathbf{t}$ are obtained:

$$\oint_c t_3 \, ds = \omega^2 \lambda U\left(\frac{x_3}{h}\right), \quad \oint_c t_1 x_1 \, ds = \frac{\omega^2 \lambda y^{11}}{2}\left(V\left(\frac{x_3}{h}\right) + W\left(\frac{x_3}{h}\right)\right),$$

$$\oint_c t_2 x_2 \, ds = \frac{\omega^2 \lambda y^{22}}{2}\left(W\left(\frac{x_3}{h}\right) - V\left(\frac{x_3}{h}\right)\right). \tag{62}$$

It is not too difficult to see that there are numerous solutions t_i to these three equations. The easiest ones to visualize are those where t_i are piecewise constant on each of the four straight segments of c.

ACKNOWLEDGMENT

The author is grateful to two of his former students, Jeffrey S. Turcotte and Peter C. Varadi, for numerous helpful discussions.

REFERENCES

1. A. E. H. LOVE 1927 *A Treatise on the Mathematical Theory of Elasticity*. Cambridge: Cambridge University Press, fourth edition.
2. W. A. GREEN 1960 in *Progress in Solid Mechanics* (I. N. Sneddon and R. Hill, editors) Vol. 1, 225–261. Dispersion relations for elastic waves in bars.
3. C. CHREE 1889 *The Quarterly Journal of Pure and Applied Mathematics* **23**, 317–342. On longitudinal vibrations.
4. R. W. MORSE 1948 *The Journal of the Acoustical Society of America* **20**, 833–838. Dispersion of compressional waves in isotropic rods of rectangular cross section.
5. R. W. MORSE 1950 *The Journal of the Acoustical Society of America* **22**, 219–223. The velocity of compressional waves in rods of rectangular cross section.
6. G. J. KYNCH and W. A. GREEN 1957 *Quarterly Journal of Mechanics and Applied Mathematics* **10**, 63–73. Vibrations of beams, I. Longitudinal modes.
7. M. G. LAMÉ 1866 *Lecons sur la Théorie Mathématique de l'Elasticité des Corps Solides*. Paris: Gauthier-Villars, second edition.
8. R. D. MINDLIN 1956 *Journal of Applied Physics* **27**, 1462–1466. Simple modes of vibration of crystals.
9. R. D. MINDLIN 1986 *International Journal of Solids and Structures* **22**, 1423–1430. On vibrations of rectangular parallelepipeds.
10. H. EKSTEIN and T. SCHIFFMAN 1956 *Journal of Applied Physics* **27**, 405–412. Free vibrations of isotropic cubes and nearly cubic parallelepipeds.
11. J. R. HUTCHINSON and S. D. ZILLMER 1983 *American Society of Mechanical Engineers Journal of Applied Mechanics* **50**, 123–130. Vibration of a free rectangular parallelepiped.
12. J. A. FROMME and A. W. LEISSA 1970 *The Journal of the Acoustical Society of America* **48**, 290–298. Free vibration of the rectangular parallelepiped.
13. A. LEISSA and Z.-D. ZHANG 1983 *The Journal of the Acoustical Society of America* **73**, 2013–2021. On the three-dimensional vibrations of the cantilevered rectangular parallelepiped.
14. C. W. LIM 1999 *The Journal of the Acoustical Society of America* **106**, 3375–3383. Three-dimensional vibration analysis of a cantilevered parallelepiped: Exact and approximate solutions.
15. M. B. RUBIN 1986 *American Society of Mechanical Engineers Journal of Applied Mechanics* **53**, 45–50. Free vibration of a free rectangular parallelepiped using the theory of a Cosserat point.
16. A. E. GREEN and N. LAWS 1966 *Proceedings of the Royal Society of London* **A293**, 145–155. A general theory of rods.
17. A. E. GREEN, N. LAWS and P. M. NAGHDI 1967 *Archive for Rational Mechanics and Analysis* **25**, 285–298. A linear theory of straight elastic rods.

18. A. E. GREEN, P. M. NAGHDI and M. L. WENNER 1974 *Proceedings of the Royal Society of London* **A337**, 485–507. On the theory of rods. II. Developments by direct approach.
19. A. E. GREEN and P. M. NAGHDI 1979 *International Journal of Solids and Structures* **15**, 829–853. On thermal effects in the theory of rods.
20. P. M. NAGHDI 1982 in *Proceedings of the IUTAM Symposium on Finite Elasticity, Bethlehem PA* 1980 (D. E. CARLSON and R. T. SHIELD, editors), 47–104. The Hague: Martinus Nijhoff. Finite deformation of elastic rods and shells.
21. A. E. GREEN and P. M. NAGHDI 1995 *Proceedings of the Royal Society of London* **A448**, 357–377. A unified procedure for the construction of theories of deformable media II. Generalized continua.
22. J. S. TURCOTTE 1996 *Approximate Theories of Elastic Rods with Applications*. Ph. D. Dissertation, University of California at Berkeley. (UMI Dissertation Number AAT 9723227).
23. S. KRISHNASWAMY and R. C. BATRA 1998 *Journal of Sound and Vibration* **215**, 577–586. On extensional vibration modes of elastic rods of finite length which include the effect of lateral deformation.
24. S. KRISHNASWAMY and R. C. BATRA 1998 *Mathematics and Mechanics of Solids* **3**, 277–295. On extensional oscillations and waves in elastic rods.
25. S. KRISHNASWAMY and R. C. BATRA 1998 *Mathematics and Mechanics of Solids* **3**, 297–301. Addendum to "On extensional oscillations and waves in elastic rods."
26. R. D. MINDLIN and G. HERRMANN 1952 in *Proceedings of the First U.S. National Congress of Applied Mechanics*-1951, 187–191 and 233. A one-dimensional theory of compressional waves in an elastic rod.
27. N. M. KINKAID, O. M. O'REILLY and J. S. TURCOTTE 2001 *American Society of Mechanical Engineers Journal of Applied Mechanics*. On the steady motions of a rotating elastic rod, to appear.
28. T. R. NORDENHOLZ and O. M. O'REILLY 1997 *International Journal of Solids and Structures* **34**, 1123–1143 and 3211–3212. On steady motions of an elastic rod with application to contact problems.
29. M. LEVINSON and D. W. COOKE 1982 *Journal of Sound and Vibration* **84**, 319–326. On the two frequency spectra of Timoshenko beams.
30. O. M. O'REILLY and J. S. TURCOTTE 1996 *Journal of Sound and Vibration* **198**, 517–521. Another mode of vibration in a Timoshenko beam.
31. M. B. RUBIN 1996 *Journal of Elasticity* **44**, 9–36. Restrictions on nonlinear constitutive relations for elastic rods.
32. R. D. MINDLIN and H. DERESIEWICZ 1955 in *Proceedings of the Second U.S. National Congress of Applied Mechanics*-1954, 175–178. Timoshenko's shear coefficient for flexural vibrations of beams.
33. P. M. NAGHDI and M. B. RUBIN 1989 *International Journal of Solids and Structures* **25**, 249–265. On the significance of normal cross-sectional extension in beam theory with application to contact problems.
34. O. M. O'REILLY 1998 *International Journal of Solids and Structures* **35**, 1009–1024. On constitutive relations for elastic rods.
35. S. WOLFRAM 1991 *Mathematica: A System for Doing Mathematics by Computer*. Redwood City, CA: Addison-Wesley.
36. M. RUMERMAN and S. RAYNOR 1971 *Journal of Sound and Vibration* **15**, 529–543. Natural frequencies of finite circular cylinders in axially symmetric longitudinal vibrations.
37. H. D. MCNIVEN and D. C. PERRY 1962 *The Journal of the Acoustical Society of America* **34**, 433–437. Axially symmetric waves in finite, elastic rods.